

Ormeloxifene nanotherapy for cervical cancer treatment

This article was published in the following Dove Press journal:
International Journal of Nanomedicine

Neeraj Chauhan^{1,2}
Diane M Maher³
Bilal B Hafeez^{1,2}
Hassan Mandil¹
Man M Singh⁴
Murali M Yallapu^{1,2}
Meena Jaggi^{1,2}
Subhash C Chauhan^{1,2}

¹Department of Pharmaceutical Sciences, University of Tennessee Health Science Center, Memphis, TN 38163, USA;

²Department of Immunology and Microbiology, School of Medicine, University of Texas Rio Grande Valley, McAllen, TX 78504, USA; ³Sanford Research Center, USD, Sioux Falls, SD 57104, USA; ⁴Research and Development, Saraswati Dental College, Lucknow, Uttar Pradesh, India

Background: Cervical cancer (CxCa) ranks as the fourth most prevalent women-related cancer worldwide. Therefore, there is a crucial need to develop newer treatment modalities. Ormeloxifene (ORM) is a non-steroidal, selective estrogen receptor modulator (SERM) that is used as an oral contraceptive in humans. Recent investigations suggest that ORM exhibits potent anti-cancer activity against various types of cancers. Nanoparticulates offer targeted delivery of anti-cancer drugs with minimal toxicity and promise newer approaches for cancer diagnosis and treatment. Therefore, the nanotherapy approach is superior compared to traditional chemotherapy, which is not site-specific and is often associated with various side effects.

Methods: Pursuing this novel nanotherapy approach, our lab has recently developed ORM-loaded poly [lactic-co-glycolic acid] (PLGA), an FDA-approved biodegradable polymer, nanoparticles to achieve targeted drug delivery and improved bioavailability. Our optimized PLGA-ORM nanoformulation showed improved internalization in both Caski and SiHa cell lines. Additionally, we employed MTS and colony forming assays to determine the short- and long-term effects of PLGA-ORM on these cells.

Results: Our results showed that this formulation demonstrated improved inhibition of cellular proliferation and clonogenic potential compared to free ORM. Furthermore, the PLGA-ORM nanoformulation exhibited superior anti-tumor activities in an orthotopic cervical cancer mouse model than free ORM.

Conclusion: Collectively, our findings suggest that our novel nanoformulation has great potential for repurposing the drug and becoming a novel modality for CxCa management.

Keywords: CxCa, ORM, PLGA, nanoformulation

Introduction

Cervical cancer (CxCa) is a cancer that starts in the cervix and is the fourth most common type of cancer in women globally. Since it develops over time, it is preventable. The American Cancer Society estimated that about 13,170 new cases of cervical cancer diagnosis and 4,250 deaths from this disease to occur in 2019 in the United States.¹ Cervical cancer is highly associated with persistent human papillomavirus (HPV) infection.² Efficient preventative measures such as HPV vaccines and Pap screening tests³ offer a continuous annual decline of ~2% in death rate. The Pap screening test detects cervical abnormalities, so can be used for early treatment modalities. HPV infection is very common in women and almost every woman is exposed to this viral infection once in her lifetime, but few will develop this dangerous malignancy.^{2,4} Often, the HPV infection is cleared by the immune system of the female

Correspondence: Meena Jaggi; Subhash C Chauhan
Department of Immunology and Microbiology, School of Medicine, University of Texas Rio Grande Valley, McAllen, TX 78504, USA
Tel +1 956 296 1926; +1 956 296 5000
Email meena.jaggi@utrgv.edu; subhash.chauhan@utrgv.edu

body, but in cases where infection persists and remains untreated, this results in the development of cancerous lesions.^{5,6} HPV alone is not enough to drive the disease, it needs some additional co-factors, namely tobacco use, an active sexual life with multiple partners, early sexual onset, poor hygiene, and low socioeconomic status, which collectively lead to the progression of cervical cancer.^{7–9} Currently, surgery, cisplatin-based chemotherapy, and radiation are the conventional methods of controlling this malignancy,^{10,11} but these modalities in general have their own limitations, such as widespread systemic toxicity, drug resistance, and poor bioavailability.^{12,13} To overcome these limitations, it becomes imperative to develop novel, improved therapeutic regimens. In this regard, a safer and faster implementation of an effective therapeutic regimen lies in discovering new uses of a drug which has already been approved for another indication.¹⁴ This is referred to as “Repurposing Drugs” that are already approved and used to treat other medical conditions in clinical practice.¹⁵

Ormeloxifene (ORM) is a non-hormonal, non-steroidal, anti-estrogen oral contraceptive agent formulated for human consumption. This is a selective estrogen receptor modulator (SERM) which inhibits the estrogen receptor (ER) in uterus, cervix, ovary, and breast while promoting ER in other organs such as bones.^{16,17} Previous studies from our and other labs demonstrate that ORM has strong anti-cancer properties against a variety of cancers, including ovarian, prostate, pancreatic, breast, and head and neck.^{18–23} Our recent study delineates the molecular mechanism of anti-cancer activity of ORM against cervical cancer.²⁴ This investigation suggested that ORM effectively inhibited cell growth and induced apoptosis in cervical cancer. Moreover, in this investigation, ORM decreased HPV-related oncogenesis and showed excellent radio-sensitization and tumor inhibitory properties. Thus, it is anticipated that ORM is highly important and effective, and sustained delivery using nanoformulations can improve its therapeutic index. Therefore, this study was directed toward examining effective ORM nanotherapy against cervical cancer.

Nanotherapy is a newer therapeutic approach that has great success in comparison with traditional chemotherapy and radiation.^{25,26} Nanoparticle formulations provide targeted delivery of drugs along with improved bioavailability in the system,²⁷ thus, are attractive tools for evolving newer treatment platforms for cancer.²⁸ Free drugs are not site-specific when delivered to the body, while the modern nanoparticle methodology facilitates site-specific, targeted delivery of drugs.¹² Due to the leaky vasculature of the tumor and the

enhanced permeation and retention (EPR) effect,²⁹ nanodrugs having the ideal size can be entrapped and specifically accumulated into tumors.³⁰ Particle sizes that are less than 5–10 nm are rapidly cleared by kidneys,^{31,32} while particle sizes around 15–100 nm tend to accumulate in liver and spleen.^{33,34} The ideal nanoparticles for cancer therapy have a suggested size range of 100–300 nm,³⁵ and this is where the EPR effect is achieved. Thus, size is the most important consideration while designing a nanomedicine, as this parameter decides the fate of the nanoparticle’s cellular uptake³⁶ and biodistribution.^{31,37} We and other researchers have shown that using poly(lactic-co-glycolic acid) (PLGA), an FDA-approved biodegradable and biocompatible polymer, in the formulation of nanoparticles to deliver chemotherapeutic drugs results in significant improvements in the inhibition of tumor burden in a wide variety of cancer models.^{38,39}

Hence, in this present study, we tested our previously developed PLGA-based ORM nanoformulation⁴⁰ for improved anti-proliferative and anti-tumor effects in cervical cancer. Our results indicated that the PLGA-ORM formulation was stable with whole human serum up to 48 hrs. This nanoformulation showed internalization in Caski and SiHa cervical cancer cells in concentration and energy-dependent manners, as confirmed by flow cytometry and fluorescent microscopy. The cellular uptake of PLGA-ORM nanoparticles followed an endocytosis-mediated pathway in cervical cancer cell lines. PLGA-ORM nanoparticles demonstrated improved anti-proliferative properties and decreased mitochondrial membrane potential compared to free ORM. Moreover, our PLGA-ORM nanoformulation showed excellent anti-tumor effects in a cervical cancer orthotopic mouse model.

Materials and methods

Chemicals

All chemicals and reagents were purchased from Sigma Aldrich Corporation (St. Louis, MO, USA) and all other cell culture consumables were purchased from Corning Life Sciences (Tewksbury, MA, USA) unless otherwise mentioned. Information regarding ormeloxifene (ORM) was kindly provided by Dr Man M. Singh.

Cell culture

Caski (ATCC[®] CRL-1550[™], cervical cancer cells derived from metastatic site of small intestine) and SiHa (ATCC[®] HTB-35[™], grade II, squamous cell carcinoma) cervical cancer cell lines were obtained from American Type

Culture Collection (ATCC) (Manassas, VA, USA). SiHa cell line was cultured in DMEM supplemented with 4500 mg/L glucose, 4 mM L-glutamine, 10% heat-inactivated FBS (Atlantic Biologicals, Lawrenceville, GA, USA), 5 mL sodium pyruvate, 5 mL nonessential amino acids, and 5 mL 1X anti-biotic/anti-mycotic (Sigma, St. Louis, MO, USA). Caski cell line was grown in RPMI medium containing 2.05 mM L-glutamine, 10% heat-inactivated FBS, and 5 mL 1X antibiotic/antimycotic. Both Caski and SiHa cell lines were incubated at 37°C in a humidified atmosphere of 5% CO₂.

Preparation and physicochemical characterization

Using a nano-precipitation method, ORM-loaded PLGA nanoformulation was prepared (Figure 1) as described in our previous study.⁴⁰ Briefly, 90 mg PLGA (50:50 lactide-glycolide ratio; inherent viscosity 1.32 dL/g at 30°C, Birmingham Polymers, Pelham, AL, USA) and 20 mg ORM were each dissolved in 5 mL acetone (≥ 99.5 , ACS reagent grade, Sigma Chemical Co., St. Louis, MO, USA) separately, then combined and the solution was added dropwise to 20 mL of aqueous 1% poly(vinyl alcohol) (PVA) (M.W. 30,000–70,000, Sigma Chemical Co., St. Louis, MO, USA) solution over 10 mins under constant stirring

with a magnetic stir plate at 500 rpm. This suspension was stirred overnight at room temperature in a chemical fume hood in order to completely evaporate the acetone. The next day, 10 mg poly(L-lysine) (PLL) (M.W. 30,000–70,000, Sigma Chemical Co., St. Louis, MO, USA) in 5 mL water was added to this suspension and allowed to stir for additional 6 hrs. The large and unbound particles were removed by centrifugation for 10 mins at 2000 rpm (Eppendorf AG centrifuge, Hamburg, Germany). Then, PLGA-ORM nanoparticles were recovered by ultracentrifugation at 30,000 rpm for 2 hrs at 4°C using a Rotor 30.50 on an Avanti J-30I Centrifuge (Beckman Coulter, Fullerton, CA, USA) and resuspended in ultra-purified water. This resulting PLGA-ORM nanoformulation was then lyophilized using the Labconco Freeze Dry System (-48°C , 133×10^{-3} mBar; Labconco, Kansas City, MO). The lyophilized PLGA-ORM was stored at 4°C for further studies. Blank (control) PLGA nanoparticles were also prepared using the same protocol but without ORM. The PLGA-ORM formulation was also analyzed for its physicochemical properties as described earlier,⁴⁰ mainly for (a) particle size using a dynamic light scattering (DLS; also known as photon correlation spectroscopy) system using Zetasizer Nano ZS90 (Malvern Instruments, Westborough, MA, USA) equipped with 50 mW diode laser as a source of light operating at

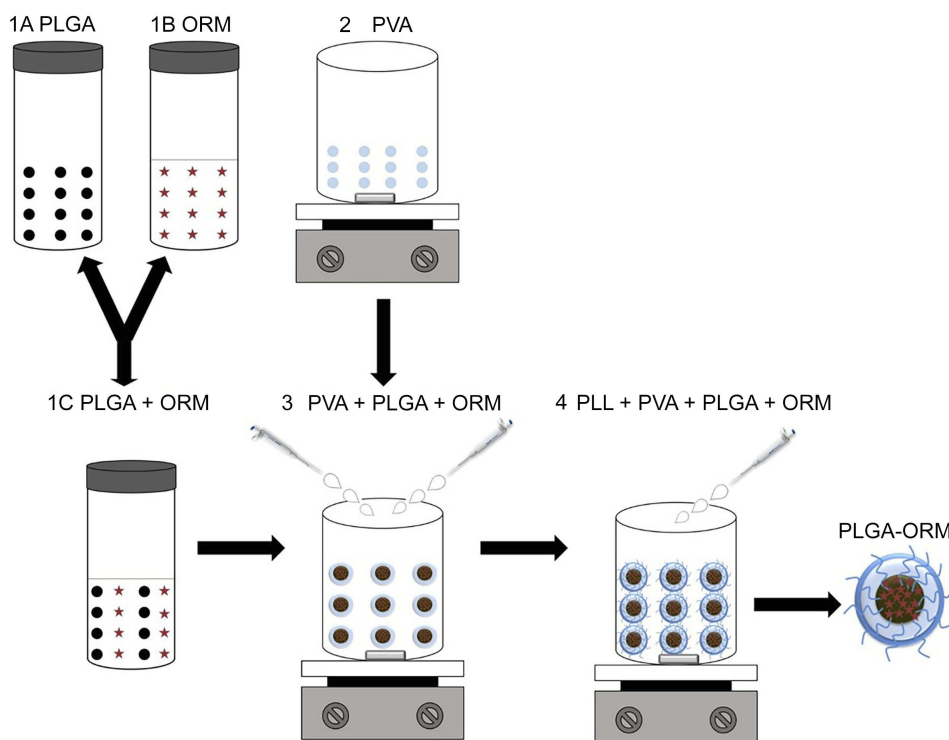


Figure 1 A schematic diagram showing the step-by-step preparation method (nano-precipitation) of the PLGA-ORM nanoformulation.

532/633 nm, and transmission electron microscope (TEM; JEOL Ltd., Tokyo, Japan), (b) chemical composition using Fourier transform infrared (FT-IR) spectroscopy (Perkin-Elmer Spectrum BX, Perkin-Elmer Inc., Norwalk, CT, USA). An average of 32 scans at a speed of 2 cm^{-1} per second ranging from 4000 to 650 cm^{-1} were presented in this study as the FT-IR spectra, (c) thermal analysis utilizing a differential scanning calorimeter (DSC 2010; TA Instruments, New Castle, DE, USA) acquired in nitrogen atmosphere at the flow rate of 50 mL/min from 0°C to 200°C with the heating rate of 5°C/min , and (d) drug loading using an UltiMate high-performance liquid chromatograph (Dionex Corporation, Sunnyvale, CA, USA) before being tested in further in vitro and in vivo experiments.

Colloidal stability of nanoparticles

Before testing nanoparticles in vivo, it is important to confirm in vitro stability of nanoparticles with human serum.⁴¹ If nanoparticles are not compatible with serum, they aggregate and result in higher absorbance value. To study human serum compatibility of our formulation, we utilized a spectrophotometer absorption method as due to the turbidity of the serum, dynamic light scattering is not very useful for authentication. For this experiment, PLGA-ORM was prepared at 1 mg/mL concentration; from this stock solution, we incubated $100\text{ }\mu\text{L}$ of this novel formulation with $100\text{ }\mu\text{L}$ of whole human serum albumin at 37°C at different time points from 0 hr to 48 hrs . At each time point, absorbance was measured at $\lambda_{\text{max}} 560\text{ nm}$ utilizing a Cytation 3 imaging multi microplate reader (BioTek, Winooski, VT, USA).

Hemocompatibility of PLGA-ORM nanoparticles

In order to evaluate the blood compatibility of PLGA-ORM, we performed a hemolysis study. For this study, 5 mL red blood cells were kindly provided by Dr Santosh Kumar's Lab (UTHSC, Memphis, purchased at the Interstate Blood Bank, Memphis, TN) which were resuspended in 10 mL phenol red free RPMI 1640 growth media. One hundred microliter red blood cells were taken in Eppendorf tubes and treated with different concentrations ($10, 50, 100, 250$ and $500\text{ }\mu\text{M}$) of free ORM and PLGA-ORM for 2 hrs at 37°C . After the incubation, red blood cells were centrifuged at 1000 rpm for 5 mins and the supernatant was measured at $\lambda_{\text{max}} 570\text{ nm}$ for optical density by a spectrophotometer. SDS and PBS were used as positive and negative controls, respectively. Results were normalized to SDS. For microscopic visualization, a drop of red

blood cells after the treatment was placed on glass slide and imaged at $200\times$ with a phase contrast microscope.

Cellular internalization of PLGA-ORM

In order to determine the cellular uptake of nanoparticles in cervical cancer cells, we incorporated 5 mg coumarin 6 green fluorescent dye to our PLGA-ORM formulation (PLGA-ORM C6) following our previous protocol.⁴⁰ A total of $200,000$ cells were seeded in a 6-well plate and allowed to attach overnight. The next morning, cells were treated with different concentrations (10 and $25\text{ }\mu\text{M}$) of coumarin 6-labeled PLGA-ORM, and its vehicle control PLGA, for 1 hr , then washed twice with PBS and plates were imaged with a fluorescent microscope (Nikon Eclipse, Melville, NY, USA). Afterward, these cells were trypsinized, washed with PBS, and collected for uptake measurement by flow cytometer. Fluorescence levels from dye containing PLGA-ORM in cells were measured under FL1 channel using Accuri C6 flow cytometer (BD Biosciences, CA, USA).

Cell association study

Both cell lines were plated ($300,000$ cells/dish) in a 60 mm dish for overnight attachment. The next day, cells were pre-incubated either at physiological temperature (37°C) or at cold temperature (4°C) for an hour before drug treatment. After an hour, cells were exposed to coumarin 6-labeled PLGA-ORM nanoparticles at $25\text{ }\mu\text{M}$ concentration for an additional hour. Next, cells were washed twice with PBS, trypsinized, centrifuged, collected in PBS, and analyzed with Accuri BD C6 flow cytometer in FL1 channel.

Cellular uptake mechanism

For this analysis, both cell lines Caski and SiHa were seeded at 2×10^5 /well in a 6-well format plate and allowed to attach overnight. The next morning, cells were pre-treated with different endocytosis pathway inhibitors such as genistein (caveolae-mediated endocytosis at $200\text{ }\mu\text{M}$), amiloride (micropinocytosis endocytosis at 10 mM), nocodazole (microtubule-mediated endocytosis at $20\text{ }\mu\text{M}$), chlorpromazine (clathrin-mediated endocytosis at $10\text{ }\mu\text{g/mL}$), and methyl- β -cyclodextrin ($\text{M}\beta\text{CD}$) (lipid rafts-mediated endocytosis at 10 mM) for 1 hr . Thereafter, cells were exposed to $25\text{ }\mu\text{M}$ of coumarin 6-labeled PLGA-ORM nanoparticles for next 1 hr at 37°C . After an hour, cells were washed twice with PBS, trypsinized, centrifuged, collected in PBS, and analyzed with Accuri BC C6 flow cytometer in the FL1 channel. We also confirmed the uptake mechanism with confocal microscopy. For this experiment, cells were plated in 4-well chamber slides

and allowed to attach overnight and next morning treated with above mentioned treatment conditions, processed for immunofluorescence and imaged at 200X.

Cell proliferation

Both Caski and SiHa (5000 cells/well) cervical cancer cell lines were seeded in 96-well plates and allowed to attach overnight. The following day, cells were treated with different micromolar concentrations of free ORM and PLGA-ORM (10, 20 and 25 μ M) and were incubated for 48 hrs. The assay was performed by utilizing an MTS CellTiter96 Aqueous One Solution (Promega Corporation, Madison, WI). At the end of the indicated time point, 20 μ L MTS reagent was added to each well and incubated at 37°C for the next 2–3 hrs. The absorbance was measured at λ_{max} 490 nm by using a microplate spectrophotometer. The experiment was done in duplicates and repeated three separate times. Data were compared to vehicle controls.

Real-time cell proliferation kinetic assay

The xCELLigence system was used to evaluate the effects of PLGA-ORM on real-time cellular proliferation/growth kinetics. The xCELLigence system is an electrical impedance-based method that provides real-time proliferation measurements. For this experiment, we used E plate VIEW 16 plates (ACEA Biosciences, San Diego, CA, USA), which were pre-incubated with 30 μ L media for 30 mins at 37°C for the background measurement. After 30 mins, Caski and SiHa cells were plated at 8×10^3 /chamber in 100 μ L media with drug treatments (20 μ M ORM and PLGA-ORM) included. Plates were incubated in the xCELLigence instrument chamber at 37°C with 5% CO₂ for real-time cell proliferation analysis. The experiment was done twice.

Colony formation assay

Caski and SiHa cell lines were seeded at 500/well in 6-well plates and allowed to adhere overnight. The following day, cells were treated with 2.5, 5 and 10 μ M of free ORM and PLGA-ORM and their respective vehicle controls and maintained for another 12–14 days. On the 14th day, cells were washed with PBS, fixed with ice-cold methanol, stained with hematoxylin (Thermo Fisher, MA, USA), and washed with water. Colonies that were visible (~50 cells) were counted manually and compared to the vehicle controls ETOH and PLGA to obtain the result. Images were captured using UVP 810 software (UVP BioSpectrum 810

Imaging System, Upland, CA, USA). The experiment was done in duplicate and repeated three independent times.

Mitochondrial membrane potential ($\Delta\Psi$ M) by TMRE

Both Caski and SiHa cell lines were plated at 200,000/well in 6-well plates and allowed to attach overnight. The next day, cells were exposed to ORM and PLGA-ORM at 25 μ M concentration along with their vehicle controls for 24 hrs. At the indicated time point, cells were trypsinized, washed, and centrifuged, then the final pellet was resuspended in 1 mL PBS containing 50 nM TMRE stain. Cells were incubated with TMRE for 30 mins in the dark at room temperature. After the incubation was completed, cells were analyzed using a BD Accuri C6 flow cytometer under the FL2 channel. The experiment was repeated three independent times.

In vivo orthotopic tumor study

Four- to six-weeks-old nu/nu female mice were purchased from Jackson Laboratory and maintained in a pathogen-free environment. This mouse model was used to develop our cervical cancer orthotopic system for this study, and all procedures were carried out as approved by the UTHSC Institutional Animal Care and Use Committee (UTHSC IACUC, Memphis, TN, USA). A total of 5×10^6 Caski cervical cancer cells per mouse were suspended in PBS and matrigel (BD Bioscience) at a 1:1 ratio. One hundred microliters of this cell suspension per mouse was directly injected to the cervix of these mice. Mice were monitored periodically for the development of tumors. Once the tumor size reached around 100 mm³, we started our treatment regimen. 100 μ g/mouse (the concentration/dose was chosen based upon our previous study)¹⁹ of PLGA-ORM and PLGA alone (vehicle control) was given to these mice intraperitoneally (i.p.) thrice weekly. Tumor volumes were calculated using the formula of tumor volume (mm³)= $\pi/6 \times L \times W \times H$ twice a week and mice survival data were also recorded by Kaplan–Meir analysis until the end of the experiment. Mice were euthanized on the 40th day after the treatment onset and tumors were observed, dissected, and weighed for future analyses.

Immunohistochemical analysis

Slides of five micron sections were prepared for immunohistochemistry from the dissected tumors after the mice experiment was completed. Slides were then deparaffinized, rehydrated, treated with hydrogen peroxide (0.3%), heat retrieved, blocked with background sniper

(Biocare Kit, Biocare Medical, Pacheco, CA, USA), and probed with primary antibodies such as HPV E6/E7 (1:50, Santa Cruz Biotechnology, Inc., Santa Cruz, CA, USA), Ki-67 and Caspase 3 cleaved (1:100, Cell Signaling Technology Inc., Danvers, MA, USA). Further, a MACH 4 HRP polymer detection kit (Biocare Kit, Biocare Medical, Pacheco, CA, USA) and a 3,3'-diaminobenzidine (DAB) substrate kit (Vector Laboratories, Burlingame, CA, USA) were used to detect the expression of the aforementioned molecules. Next, slides were counterstained with hematoxylin, dehydrated, and mounted with VectaMount (Vector Laboratories, Burlingame, CA, USA). Slides were further imaged and scanned at the Department of Pathology and Laboratory Medicine at UTHSC, Memphis, TN, USA.

Statistical methods

The data are presented as mean±standard error (SEM) in this study. Statistical analyses were done by using an unpaired, two-tailed student's *t*-test. The results were considered significant if *p*-values<0.05. All graphs were generated using GraphPad Prism (5.03, GraphPad Software, Inc., La Jolla, CA, USA).

Results

Physicochemical characterization of PLGA-ORM

The PLGA-ORM nanoformulation was prepared when required for the described experiments following our published protocol.⁴⁰ After preparation, particle size, FT-IR spectra, thermal analysis, and drug loading were evaluated to confirm the product consistency with our protocol. DLS data revealed that the PLGA-ORM particle size was around ~250 nm and the drug content was found to be around ~80% by HPLC analysis (Figure 2A) which was in accordance with previously published studies on PLGA nanoformulations from our and other groups.^{38,40,42} TEM images of PLGA-ORM nanoparticles indicated that the formed particles were spherical in shape, with well-dispersed stage (Figure 2B). FT-IR (Figure 2C) and DSC (Figure 2D) analyses indicated that ORM was completely miscible with PLGA nanoparticles, which suggested its superior encapsulation into the polymer matrix. These findings were in accordance with our previously published data.³⁹

Serum stability and hemocompatibility of PLGA-ORM

Nanoparticles can easily aggregate, disintegrate, or leak the drug upon their in vivo administration when particles encounter systemic blood/serum. Therefore, it becomes necessary to evaluate the stability of nanoparticles in contact with serum.⁴³ We utilized whole human serum albumin to assess the stability of our PLGA-ORM nanoformulation. Results from the absorption method indicated that this formulation is highly stable with human serum, as confirmed by no or negligible change in absorbance (Figure 2E). Higher absorbance value is indicative of a higher degree of aggregation. We also evaluated the toxicity profile or hemocompatibility of PLGA-ORM with human red blood cells at different concentrations (10–500 μM) (Figure 3A–C) where we used sodium dodecyl sulfate (SDS, 500 μM) as positive control and phosphate buffer saline (PBS, 500 μM) as negative control. SDS caused significant cell death while PBS showed no signs of hemotoxicity. ORM and PLGA-ORM also showed a dose-dependent response to RBCs (Figure 3A–C).

PLGA-ORM nanoparticles internalize in cervical cancer cells

Measuring the in vitro cellular internalization of nanoparticles is an essential experiment. A green dye (coumarin 6) was tagged to PLGA-ORM nanoparticles for visual tracking in cells in the uptake process. Both fluorescent microscope and flow cytometer measurements^{44,45} were performed to determine the cellular uptake pattern of PLGA-ORM nanoparticles in cervical cancer cells. The microscopic images and flow cytometer data revealed that particles were being taken up by Caski and SiHa cell lines (Figure 4A and B) in dose-dependent manner. Fluorescent images suggested that PLGA-ORM was primarily located in the cytoplasm of these cells. Temperature is an important factor that facilitates the uptake of particles. In some cases, particle uptake is energy/temperature dependent. Thus, we conducted a flow cytometry study at two different temperatures. The results from this experiment showed that at 4°C, the particle uptake was blocked, whereas at 37°C physiological temperature, the uptake of particles was normal in both Caski and SiHa cell lines (Figure 4C).

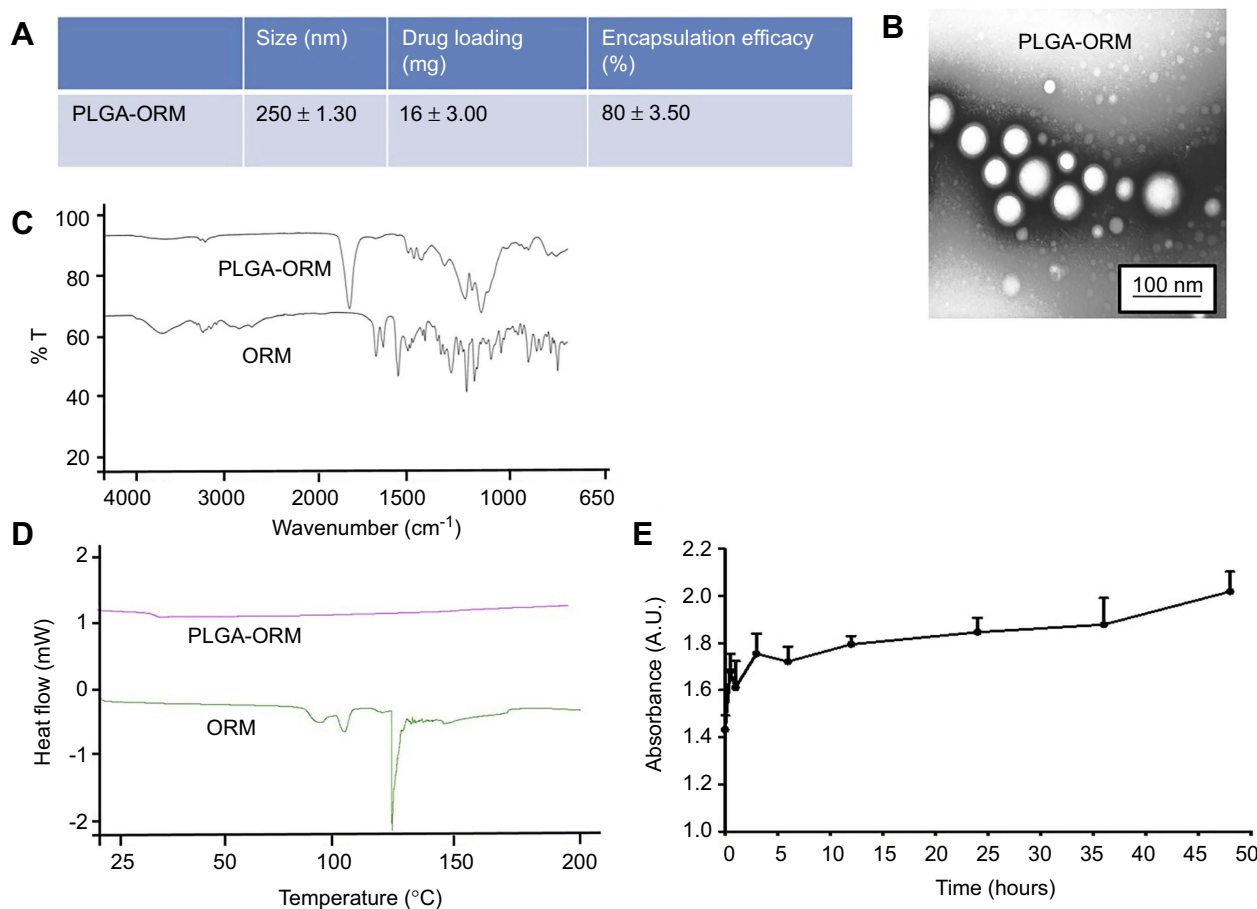


Figure 2 Physicochemical characterization of PLGA-ORM. (A) Table shows particle size (measured by DLS), drug loading, and encapsulation efficiency. (B) TEM image shows particle size of PLGA-ORM. Image was taken at 600,000× (C) FT-IR and (D) DSC spectra of free ORM and PLGA-ORM. (E) Whole human serum stability profile of PLGA-ORM for 48 hrs. **Abbreviations:** DLS, dynamic light scattering; DSC, differential scanning calorimeter; ORM, ormeloxifene.

PLGA-ORM nanoparticles utilize endocytosis pathways for internalization in cervical cancer cells

Endocytosis is the main pathway that nanoparticles use for internalizing into the cells. But endocytosis has various different mechanisms for cellular uptake⁴⁶ (Figure 5E). Therefore, to determine the uptake mechanism of PLGA-ORM nanoparticles, we treated Caski and SiHa cell lines with different endocytosis pathway inhibitors and performed flow cytometry analyses. Data from this experiment suggested that particles mainly utilized the lipid raft, microtubule, micropinocytosis, and caveolae-dependent pathways for their uptake into the Caski cell line (Figure 5A) over the clathrin-dependent pathway. In the SiHa cell line, particles used all five tested pathways, namely lipid raft, clathrin-dependent, microtubule, micropinocytosis, and caveolae-dependent pathways for their internalization (Figure 5B). Results were consistent with confocal images as multiple

pathways for nanoparticles' uptake were observed in both cell lines (Figure 5C and D).

PLGA-ORM decreases cell viability, clonogenic potential, and mitochondrial membrane potential of cervical cancer cells

In order to elaborate the anti-cancer properties of PLGA-ORM, we assessed an MTS assay for 48 hrs. The results showed a marked decrease in cellular viability of both Caski (Figure 6A) and SiHa (Figure 6B) cell lines when compared to free ORM. Real-time growth kinetics measured by the xCELLigence system also supported these findings (Figure 6C for Caski and Figure 6D for SiHa). We also performed a flow cytometry experiment to analyze the ability of PLGA-ORM to induce apoptosis. We used TMRE stain to detect the depolarized mitochondria, which is an indication of apoptosis induction. Our flow cytometry data revealed that PLGA-

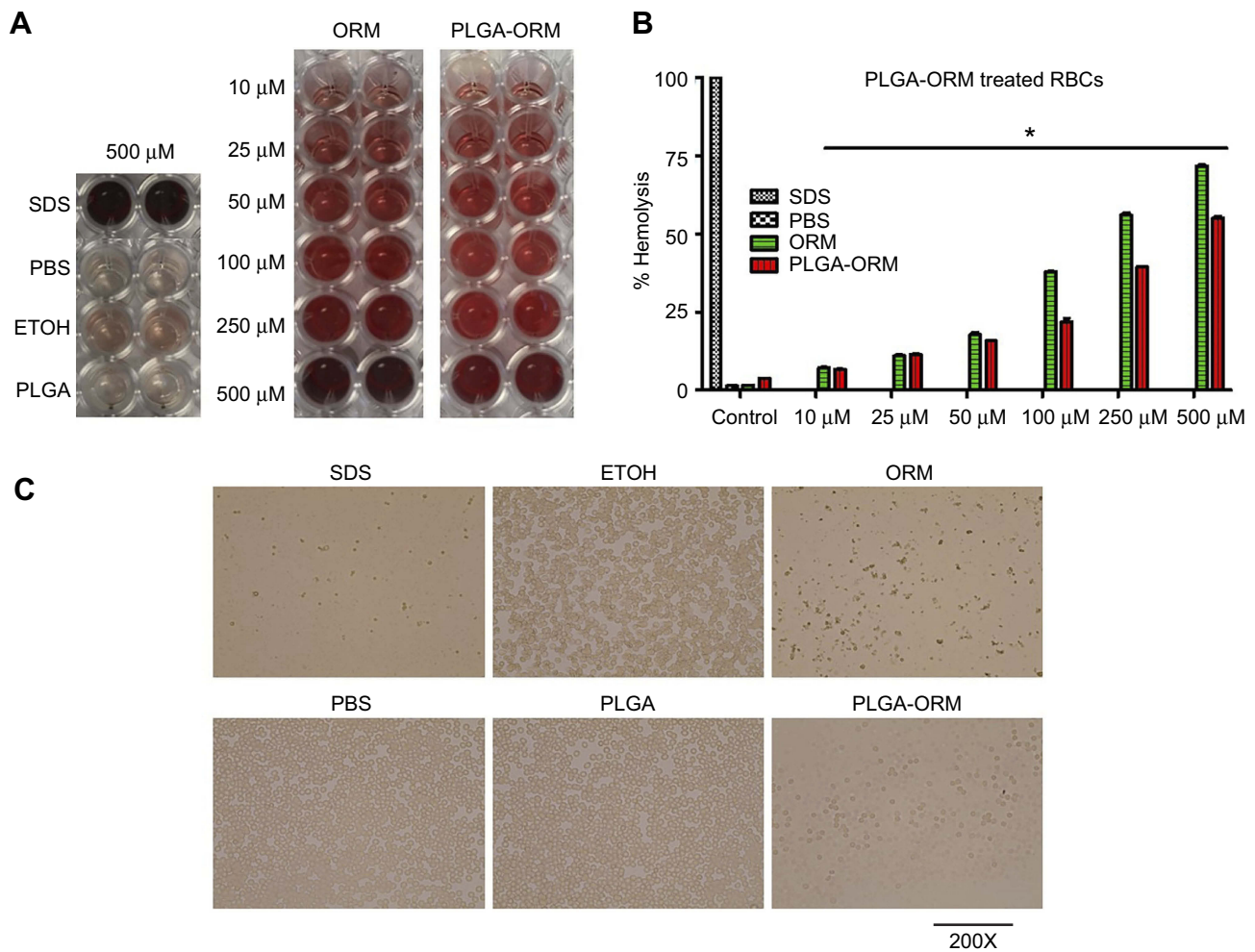


Figure 3 Hemocompatibility (Hemolysis) of PLGA-ORM with human RBCs. **(A)** Optical images of the supernatant. Human RBCs were treated with PLGA-ORM at different concentrations for 2 hrs at 37°C and centrifuged at 1000 rpm for 5 mins. Supernatant was collected in a 96-well plate and imaged with CamScanner mobile app. **(B)** Absorbance (optical density) of the supernatant. Supernatant containing wells were measured at 570 nm. SDS and PBS were used as positive and negative controls, respectively. Results were normalized to SDS. Error bars show SEM, n=3. *p<0.05. **(C)** Phase contrast images of RBCs. After 2 hrs of treatment, a drop of RBCs was placed on a glass slide, covered with coverslip and imaged with a phase contrast microscope. Images shown only at the highest concentration used (500 μM). Images were taken at 200X. **Abbreviations:** ORM, ormeloxifene; RBCs, red blood cells.

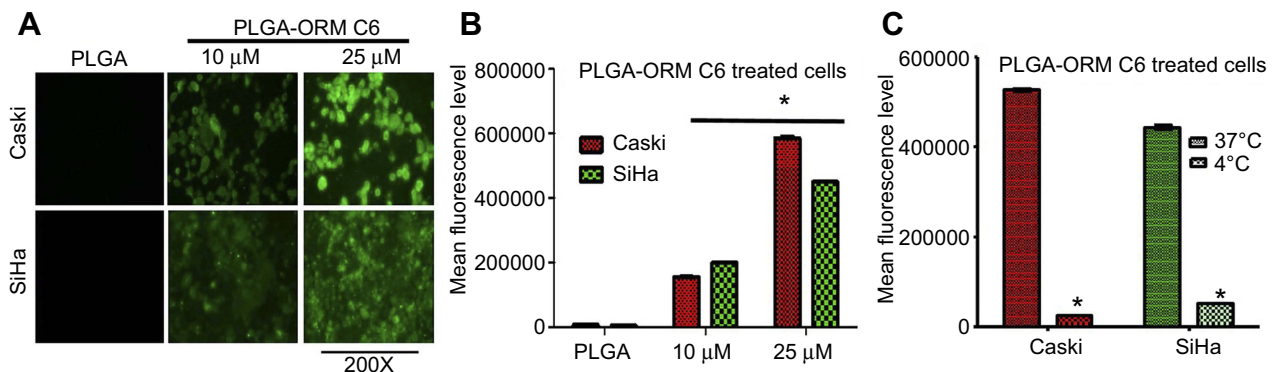


Figure 4 Cellular uptake and uptake mechanism of PLGA-ORM. **(A)** Qualitative representation of cellular uptake. Caski and SiHa cells were treated with coumarin-6-loaded PLGA-ORM nanoparticles for 1 hr. Cells indicated an increased uptake in a dose-dependent manner. Images were taken at 200X. **(B)** Quantitative measurement of PLGA-ORM uptake. Coumarin-6-loaded PLGA-ORM internalization in Caski and SiHa cell lines increased in a dose-dependent manner. Results were normalized to the PLGA control particles. Error bars show SEM, n=3. *p<0.05. **(C)** Internalization of coumarin-6-loaded PLGA-ORM C6 and incubated at different temperatures. Cells showed blocked or inhibited uptake of particles when incubated at 4°C. Results were normalized to the particles incubated at 37°C. Error bars show SEM, n=3. *p<0.05. **Abbreviation:** ORM, ormeloxifene.

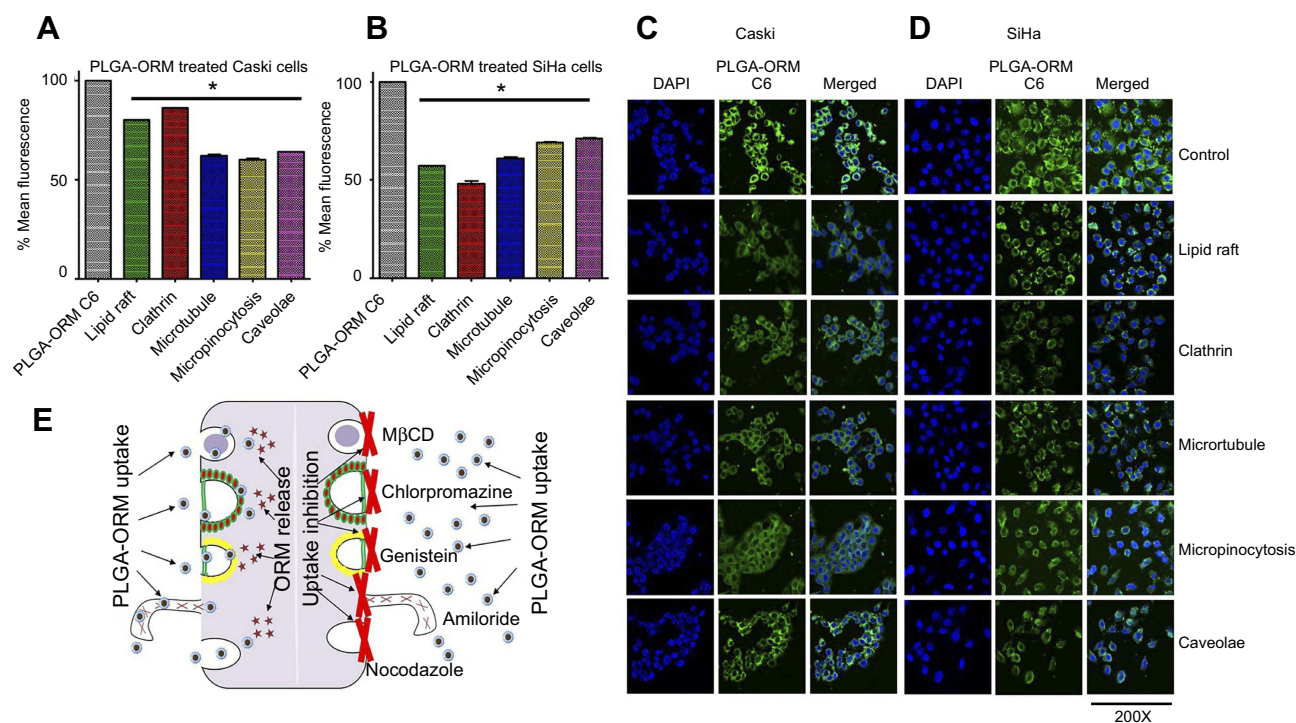


Figure 5 Internalization mechanism of PLGA-ORM nanoparticles in cervical cancer cells. **(A)** Caski and **(B)** SiHa cell lines were treated with different endocytosis pathway inhibitors and PLGA-ORM C6 for 1 hr each. Cellular uptake of PLGA-ORM was decreased with multiple inhibitors' treatment as confirmed by flow cytometer. Results were normalized to PLGA-ORM C6 particles. Error bars show SEM, $n=3$. $*p<0.05$. **(C)** Caski and **(D)** SiHa confocal images also showing that PLGA-ORM C6 internalized in cells through multiple endocytosis pathways after 1 hr treatment. Experiments were performed in the presence of endocytosis inhibitors. Images were taken at 200 \times . **(E)** A schematic showing internalization of PLGA-ORM nanoparticles in cells using endocytosis pathway.

Abbreviation: ORM, ormeloxifene.

ORM significantly reduced the mitochondrial membrane potential of both Caski (Figure 6E) and SiHa (Figure 6F) cell lines when compared to free ORM. When we performed the colony formation assay for the long-term treatment capability of PLGA-ORM, the results were even more dramatic. PLGA-ORM had an inhibitory effect on clonogenic potential of both Caski (Figure 7A and B) and SiHa (Figure 7C and D) cell lines in comparison to free ORM. Interestingly, PLGA-ORM treatment resulted in a lower number of colonies than free ORM treatment even at the lowest concentration of 2.5 μM .

PLGA-ORM nanoparticles inhibit cervical cancer tumorigenesis in orthotopic mice model

In order to evaluate anti-tumor efficacy of PLGA-ORM formulation, we developed an orthotopic mouse model of cervical cancer using the Caski cell line. We designed two groups for this study named as PLGA and PLGA-ORM with six mice in each group. HPV-positive Caski cervical cancer cells were directly injected into the cervix of female nude

mice. These mice started showing tumor development at around 2 weeks and we started the drug treatment, as the tumor size was around 100 mm^3 . PLGA-ORM and its vehicle control PLGA blank were administered (100 $\mu\text{g}/\text{mouse}$) intraperitoneally. Once the control mice tumor size reached around 1000 mm^3 , we terminated the study (on the 40th day) and mice were euthanized, then tumors were collected from both treatment groups. It was clear that PLGA-ORM reduced the overall burden of tumors (Figure 8A) and increased the survival rate in these mice when compared to its vehicle control PLGA (Figure 8B) and free ORM (data not presented in this manuscript).²³ Tumor volume (size) was measured twice a week using a digital vernier caliper and results showed that PLGA-ORM significantly decreased the tumor volume when compared to PLGA control (Figure 8C) and free ORM (data not presented in this manuscript).²⁴ Compared to the control mice group and free ORM (data not presented in this manuscript),²⁴ tumor weight was also decreased in the PLGA-ORM treated mice group (Figure 8D). Further, immunohistochemistry data, which was obtained from the dissected tumors' slides, revealed that PLGA-ORM effectively inhibited the expression of HPV

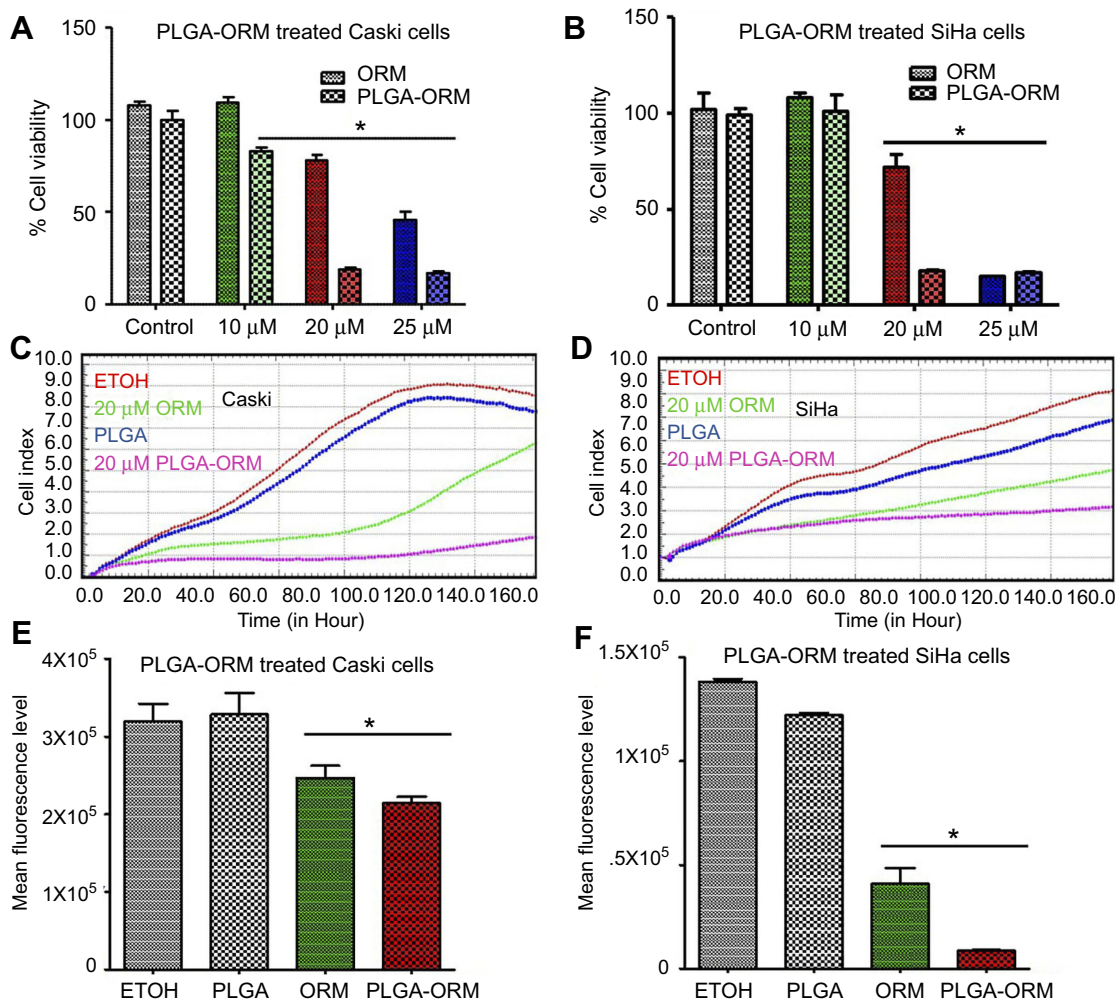


Figure 6 PLGA-ORM decreased cell proliferation and mitochondrial membrane potential of cells. Cell proliferation. (A) Caski and (B) SiHa cell lines were treated with ORM and PLGA-ORM (10, 20 and 25 μ M) for 48 hrs. MTS method was used to determine proliferation and absorbance was measured at 490 nm. Results were normalized to the vehicle controls (ETOH and PLGA) and free ORM. Error bars show SEM, n=3. * p <0.05. Growth kinetics through xCELLigence RTCA (real-time cell analysis). (C) Caski and (D) SiHa PLGA-ORM inhibited growth of Caski and SiHa cells in real time. Cells were exposed to ORM and PLGA-ORM treatments at 20 μ M concentration and then measured for real-time growth kinetics. Mitochondrial membrane potential. (E) Caski and (F) SiHa cell lines were treated with 25 μ M ORM and PLGA-ORM for 24 hrs and measured for mitochondrial membrane potential by TMRE stain using flow cytometer. Results were normalized to the vehicle controls (ETOH and PLGA) and free ORM. Error bars show SEM, n=3. * p <0.05.

Abbreviation: ORM, ormeloxifene.

E6/E7 oncoproteins and Ki-67 (a well-known proliferative marker), and enhanced the expression of the cleaved form of Caspase 3, which is the hallmark of the initiation of apoptosis (Figure 8E). These findings from the immunohistochemical analysis clearly indicated that PLGA-ORM targets oncogenic HPV E6 and E7 signaling, which is the major cause of elevated proliferation and compromised apoptosis in cervical cancer cells.⁴⁷

Discussion

Persistent high-risk HPV infection, along with other risk factors including early sexual onset and highly active sexual life, low social and economic status, and tobacco use, are the main causes of the development of cervical

cancer.^{48,49} There are several preventative and therapeutic methods for cervical cancer, depending upon the stage of the lesion.¹⁰ HPV vaccines and Pap screening are often effective for pre-cancerous lesions.^{50,51} Surgical removal of the organ, radiation, and cisplatin-based chemotherapy are the traditional clinical regimens of choice for managing cancerous lesions.¹¹ However, advanced stages of cervical cancer are difficult to treat due to drug resistance and toxicity; thus, advanced-stage cervical cancer is associated with poor 5-year survival rate and with higher mortality in females around the world.^{11,13} Therefore, newer approaches that can overcome cytotoxicity issues and at the same time provide tumor site-specific targeted delivery of the drugs are highly desirable.

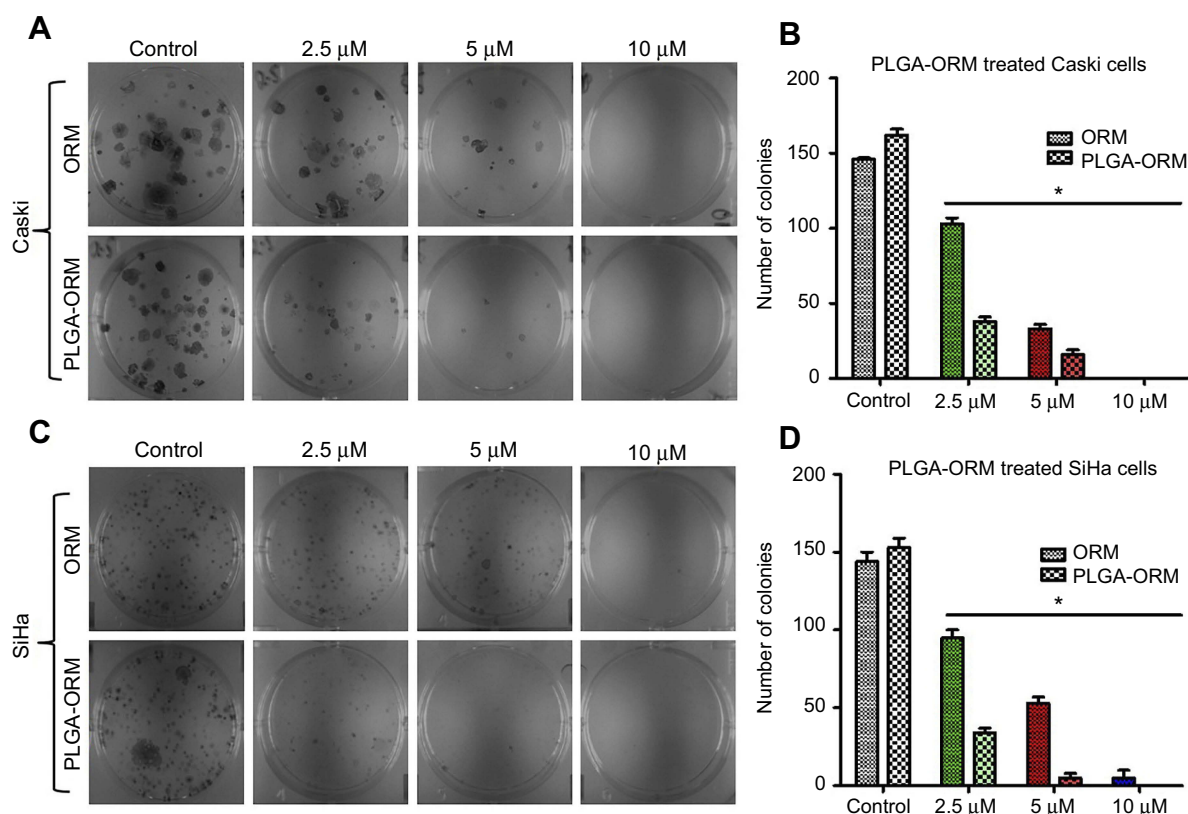


Figure 7 PLGA-ORM decreased colony forming ability of cells. Qualitative images for decreased clonogenic potential. (A) Caski and (C) SiHa cell lines were treated with ORM and PLGA-ORM (2.5, 5 and 10 μ M) for 14 days. Images were taken using a UPV 810 imaging system. Graph representation of decreased clonogenic potential. (B) Caski and (D) SiHa results were normalized to the vehicle controls (ETOH and PLGA) and free ORM. Error bars show SEM, n=3. * p <0.05.

Abbreviation: ORM, ormeloxifene.

Nanodrugs are designed in such a way that they have an ideal size range of 100–300 nm. In this size range, they specifically utilize the EPR effect in tumors to obtain enhanced and improved therapeutic outcomes.^{29,52,53} Additionally, nanodrugs allow using lower doses of anti-cancer drugs, thus keeping higher amounts of drug away from normal, healthy cells/tissues.^{25,54} Therefore, in this study, we focused on a PLGA-based ormeloxifene nanoformulation for tissue-specific delivery of the drug in cervical cancer. Ormeloxifene is an anti-estrogen, non-hormonal oral contraceptive agent for human use.^{16,55}

In the present study, an ORM-loaded PLGA nanoformulation was prepared and evaluated for its serum compatibility, cellular uptake efficacy, cellular uptake mechanism, and anti-cervical cancer properties both in vitro and in vivo. Particle size and drug loading estimations confirmed that we were successful in generating a formulation that is reproducible over the time period studied, as the results of these two were in accordance with our first, previously published paper describing PLGA-ORM.⁴⁰

The PLGA-ORM nanoformulation was found to have the particle size of around 250 nm (DLS) and less than 100 nm (TEM) (Figure 2A and B). The observed difference in measured particle sizes is mainly because DLS measures particles in solution, which causes aggregation, while TEM measures single particles. ORM was well encapsulated in the PLGA-ORM nanoformulation as indicated by FT-IR and DSC spectra (Figure 2C and D), which resulted in a superior drug loading of about 80% (Figure 2A). This nanoformulation was stable and compatible with whole human serum albumin for up to 48 hrs (Figure 2E), and with human red blood cells for 2 hrs (Figure 3A–C) which confirmed that the formulation was safe to test in further experiments. Two cell line models (Caski and SiHa) of cervical cancer were selected for the successful accomplishment of our in vitro studies. Caski and SiHa cell lines were treated with PLGA-ORM (labeled with coumarin 6 dye for fluorescent microscopic and flow cytometry evaluations) and incubated for 1 hr to determine uptake efficacy; the data revealed that PLGA-ORM displayed an improved uptake profile in a dose-dependent manner when compared with PLGA

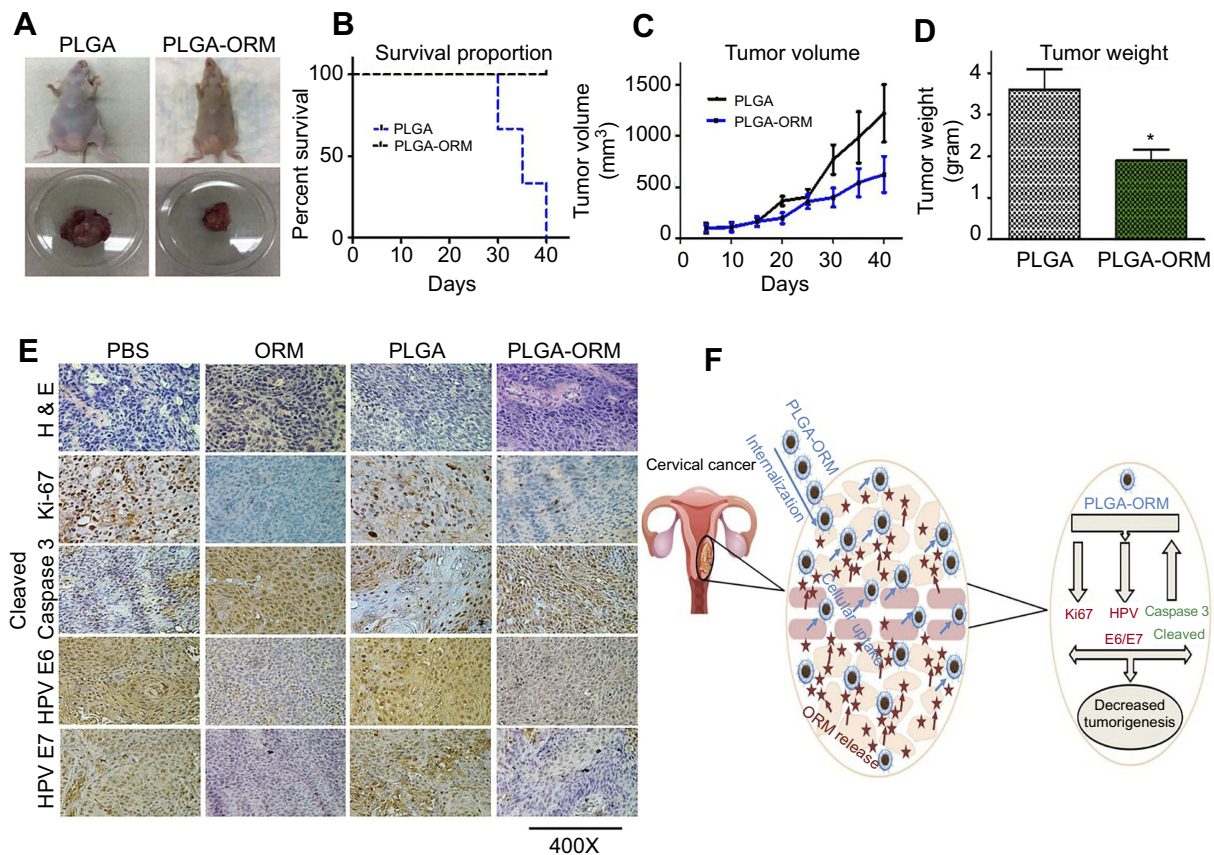


Figure 8 PLGA-ORM inhibited tumor growth of cervical cancer in orthotopic mice model. **(A)** Images represent mice from different treatment groups and their dissected tumors. **(B)** Percent survival curve for PLGA-ORM and PLGA blank treated mice. PLGA-ORM (black line) showed 100% survival in contrast to the PLGA control group. **(C)** Average tumor volume of PLGA-ORM and PLGA blank treated mice. PLGA-ORM markedly reduced the tumor volume over that of PLGA blank control. **(D)** Weight measurement for the dissected tumors. PLGA-ORM significantly reduced the tumor weight. Error bars show SEM, $n=6$, $*p<0.05$, and results were compared with vehicle control PLGA. **(E)** Immunohistochemical analysis. Images show modulated expression of different proteins involved in cervical cancer carcinogenesis. Images were taken at 400 \times . **(F)** A schematic diagram describing decreased cervical cancer tumorigenesis after PLGA-ORM treatment.

Abbreviation: ORM, ormeloxifene.

blank control (Figure 4A and B). Cell association studies also demonstrated that the cellular uptake of PLGA-ORM was energy dependent, as a drastic reduction in uptake pattern was recorded at the lower temperature of 4 $^{\circ}$ C (Figure 4C). Previously published literature suggested that it is possible that nanoparticles may obtain more than one or multiple endocytosis pathways for their uptake into the cells.⁵⁶ Further evaluation of PLGA-ORM nanoparticles' uptake mechanism showed the correlated results indicating that particle uptake was mediated through multiple endocytosis pathways in both Caski (Figure 5A and C) and SiHa (Figure 5B and D) cell lines.

Furthermore, PLGA-ORM indicated enhanced anti-proliferative efficacy in Caski and SiHa cell lines compared to free ORM and vehicle control PLGA, as validated by a cell proliferation assay for 48 hrs (Figure 6A and B). It has been already established that ORM selectively targets cancer cells and has no or minimal toxicity towards normal cells.²¹ These proliferation/growth inhibitory findings are consistent with the data obtained by

using a real-time growth kinetic assay (Figure 6C and D) and clonogenic potential assay for 14 days (Figure 7A–D). We also elucidated the ability of PLGA-ORM to decrease mitochondrial membrane potential as an indication of apoptosis cascade in the cells. PLGA-ORM treated Caski and SiHa cell lines showed a significant decrease in the membrane potential of mitochondria when compared with free ORM and PLGA blank control (Figure 6E and F).

Additionally, we developed an orthotopic cervical cancer mouse model to investigate PLGA-ORM's in vivo effects. Results from this experiment clearly exhibited superior tumor uptake of PLGA-ORM over free ORM (data not presented in this manuscript)²⁴ and its vehicle control PLGA blank (Figure 8A). Overall, the mice survival rate was significantly increased with PLGA-ORM treatment (Figure 8B) when compared to vehicle control PLGA and free ORM (data not presented in this manuscript).²⁴ In accordance with these results, tumor

volume (Figure 8C) and weight (Figure 8D) were also significantly decreased when mice were treated with PLGA-ORM compared to its vehicle control PLGA and free ORM (data not presented in this manuscript).²⁴ Furthermore, PLGA-ORM modulated the expression of key molecules involved in cervical cancer carcinogenesis, as decreased levels of HPV E6/7 and Ki-67, and increased levels of cleaved Caspase 3, were observed on the stained immunohistochemical tumor slides (Figure 8E) when compared with vehicle controls PBS, PLGA, and with free ORM. This study was primarily focused on anti-tumor effects of PLGA-ORM; however, further evaluations of this formulation are warranted to investigate the bio-distribution profile in different organs. We are in the process of investigating these parameters for our future publications.

Conclusion

In the present study, we have shown efficient delivery and therapeutic potential of our novel nanoformulation PLGA-ORM in cervical cancer for the first time. Our formulation showed great serum stability and enhanced cellular uptake in Caski and SiHa cervical cancer cell lines as compared to free ORM. Further in vitro functional studies showed that PLGA-ORM decreased cell proliferation and induced apoptosis. Additionally, PLGA-ORM exhibited successful site-specific delivery of the drug to the tumors in an orthotopic mouse model of cervical cancer. Therefore, altogether our findings suggest that the PLGA-ORM nanoformulation described herein may become a novel and efficacious therapeutic modality for the management of cervical cancer (Figure 8F).

Ethics approval

All animal experimental procedures were carried out as approved by the UTHSC Institutional Animal Care and Use Committee (UTHSC IACUC, Memphis, TN, USA). Also, UTHSC complies with the Animal Welfare Act (AWA) and the Public Health Service Policy on Humane Care and Use of Laboratory Animals and these guidelines have been followed while performing the animal experiment.

Acknowledgments

This work is financially supported by the National Institute of Health grant number [U01CA162106, R01CA142736, R01CA204552, R01CA210192, R01CA206069, and R15CA213232]. Also, Ms. Saini Setua has generously performed confocal microscopic experiments.

Author contributions

All authors contributed to data analysis, drafting and revising the article, gave final approval of the version to be published, and agree to be accountable for all aspects of the work.

Disclosure

The authors report no potential conflicts of interest in this work.

References

1. American Cancer Society [homepage on the internet]. Key Statistics for Cervical Cancer; 2019. Available from <https://www.cancer.org/cancer/cervical-cancer/about/key-statistics.html>. Accessed August 8, 2019.
2. Burd EM. Human papillomavirus and cervical cancer. *Clin Microbiol Rev.* 2003;16(1):1–17. doi:10.1128/cmr.16.1.1-17.2003
3. Reid J. Women's knowledge of Pap smears, risk factors for cervical cancer, and cervical cancer. *J Obstetric Gynecologic Neonatal Nurs.* 2001;30(3):299–305. doi:10.1111/j.1552-6909.2001.tb01548.x
4. Bosch F, Lorincz A, Munoz N, Meijer C, Shah K. The causal relation between human papillomavirus and cervical cancer. *J Clin Pathol.* 2002;55(4):244–265. doi:10.1136/jcp.55.4.244
5. Bosch FX, De Sanjosé S. Human papillomavirus and cervical cancer—burden and assessment of causality. *J National Cancer Inst Monogr.* 2003;Chapter 1(31):3–13. doi:10.1093/oxfordjournals.jnci-monographs.a003479
6. Maglennon GA, Doorbar J. The biology of papillomavirus latency. *Open Virol J.* 2012;6:1. doi:10.2174/1874357901206010190
7. Castellsagué X, Muñoz N. Cofactors in human papillomavirus carcinogenesis—role of parity, oral contraceptives, and tobacco smoking. *J Natl Cancer Inst Monogr.* 2003;31:20–28. doi:10.1093/oxfordjournals.jncimonographs.a003477
8. Brinton LA, Hamman RF, Huggins GR, et al. Sexual and reproductive risk factors for invasive squamous cell cervical cancer. *J Natl Cancer Inst.* 1987;79(1):23–30.
9. Brinton LA, Schairer C, Haenszel W, et al. Cigarette smoking and invasive cervical cancer. *Jama.* 1986;255(23):3265–3269.
10. Carter JS, Downs JLS. cervical cancer tests and treatment. *Female Patient (Parsippany).* 2011;36(1):34.
11. Janicek MF, Averette HE. Cervical cancer: prevention, diagnosis, and therapeutics. *CA Cancer J Clin.* 2001;51(2):92–114.
12. Cho K, Wang X, Nie S, Shin DM. Therapeutic nanoparticles for drug delivery in cancer. *Clin Cancer Res.* 2008;14(5):1310–1316. doi:10.1158/1078-0432.CCR-07-1441
13. Duyun A, Van Eijkeren M, Kenter G, Zwinderman K, Ansink A. Recurrent cervical cancer: detection and prognosis. *Acta Obstet Gynecol Scand.* 2002;81(8):759–763.
14. Aubé J. Drug repurposing and the medicinal chemist. *ACS Med Chem Lett.* 2012;3(6):442–444. doi:10.1021/ml300114c
15. Boguski MS, Mandl KD, Sukhatme VP. Repurposing with a Difference. *Science.* 2009;324(5933):1394–1395. doi:10.1126/science.1169920
16. Singh M. Centchroman, a selective estrogen receptor modulator, as a contraceptive and for the management of hormone-related clinical disorders. *Med Res Rev.* 2001;21(4):302–347.
17. Lal J. Clinical pharmacokinetics and interaction of centchroman—a mini review. *Contraception.* 2010;81(4):275–280. doi:10.1016/j.contraception.2009.11.007

18. Gara RK, Sundram V, Chauhan SC, Jaggi M. Anti-cancer potential of a novel SERM ormeloxifene. *Curr Med Chem.* 2013;20(33):4177. doi:10.2174/09298673113209990197
19. Maher DM, Khan S, Nordquist JL, et al. Ormeloxifene efficiently inhibits ovarian cancer growth. *Cancer Lett.* 2015;356(2):606–612. doi:10.1016/j.canlet.2014.10.009
20. Khan S, Ebeling MC, Chauhan N, et al. Ormeloxifene suppresses desmoplasia and enhances sensitivity of gemcitabine in pancreatic cancer. *Cancer Res.* 2015;75(11):2292–2304. doi:10.1158/0008-5472.CAN-14-2397
21. Srivastava VK, Gara RK, Bhatt M, Sahu D, Mishra DP. Centchroman inhibits proliferation of head and neck cancer cells through the modulation of PI3K/mTOR pathway. *Biochem Biophys Res Commun.* 2011;404(1):40–45. doi:10.1016/j.bbrc.2010.11.049
22. Singh N, Zaidi D, Shyam H, Sharma R, Balapure AK. Polyphenols sensitization potentiates susceptibility of MCF-7 and MDA MB-231 cells to centchroman. *PLoS One.* 2012;7(6):e37736. doi:10.1371/journal.pone.0037736
23. Hafeez BB, Ganju A, Sikander M, et al. Ormeloxifene suppresses prostate tumor growth and metastatic phenotypes via inhibition of oncogenic β -catenin signaling and EMT progression. *Mol Cancer Ther.* 2017;16(10):2267–2280. doi:10.1158/1535-7163.MCT-17-0157
24. Chauhan N, Maher DM, Yallapu MM, et al. A triphenylethylene nonsteroidal SERM attenuates cervical cancer growth. *Sci Rep.* 2019;9(1):10917. doi:10.1038/s41598-019-46680-0
25. Brannon-Peppas L, Blanchette JO. Nanoparticle and targeted systems for cancer therapy. *Adv Drug Deliv Rev.* 2004;56(11):1649–1659. doi:10.1016/j.addr.2004.02.014
26. Thrall JH. Nanotechnology and Medicine 1. *Radiology.* 2004;230(2):315–318. doi:10.1148/radiol.2302031698
27. Huang Q, Yu H, Ru Q. Bioavailability and delivery of nutraceuticals using nanotechnology. *J Food Sci.* 2010;75(1):R50–R57. doi:10.1111/j.1750-3841.2009.01457.x
28. Peer D, Karp JM, Hong S, Farokhzad OC, Margalit R, Langer R. Nanocarriers as an emerging platform for cancer therapy. *Nat Nanotechnol.* 2007;2(12):751–760. doi:10.1038/nmano.2007.387
29. Torchilin V. Tumor delivery of macromolecular drugs based on the EPR effect. *Adv Drug Deliv Rev.* 2011;63(3):131–135. doi:10.1016/j.addr.2010.03.011
30. Matsumura Y, Maeda H. A new concept for macromolecular therapeutics in cancer chemotherapy: mechanism of tumorotropic accumulation of proteins and the antitumor agent smancs. *Cancer Res.* 1986;46(12 Part 1):6387–6392.
31. Vinogradov SV, Bronich TK, Kabanov AV. Nanosized cationic hydrogels for drug delivery: preparation, properties and interactions with cells. *Adv Drug Deliv Rev.* 2002;54(1):135–147.
32. Choi HS, Liu W, Misra P, et al. Renal clearance of quantum dots. *Nat Biotechnol.* 2007;25(10):1165–1170. doi:10.1038/nbt1340
33. Ilium L, Davis S, Wilson C, Thomas N, Frier M, Hardy J. Blood clearance and organ deposition of intravenously administered colloidal particles. The effects of particle size, nature and shape. *Int J Pharm.* 1982;12(2–3):135–146. doi:10.1016/0378-5173(82)90113-2
34. Moghimi SM, Hedeman H, Muir I, Illum L, Davis SS. An investigation of the filtration capacity and the fate of large filtered sterically-stabilized microspheres in rat spleen. *Biochimica Et Biophysica Acta (BBA) Gen Subj.* 1993;1157(2):233–240. doi:10.1016/0304-4165(93)90105-H
35. Gaumet M, Vargas A, Gurny R, Delie F. Nanoparticles for drug delivery: the need for precision in reporting particle size parameters. *Eur J Pharmaceutics Biopharm.* 2008;69(1):1–9. doi:10.1016/j.ejpb.2007.08.001
36. Conner SD, Schmid SL. Regulated portals of entry into the cell. *Nature.* 2003;422(6927):37–44. doi:10.1038/nature01451
37. Manjunath K, Venkateswarlu V. Pharmacokinetics, tissue distribution and bioavailability of clozapine solid lipid nanoparticles after intravenous and intraduodenal administration. *J Controlled Release.* 2005;107(2):215–228. doi:10.1016/j.jconrel.2005.06.006
38. Yallapu MM, Gupta BK, Jaggi M, Chauhan SC. Fabrication of curcumin encapsulated PLGA nanoparticles for improved therapeutic effects in metastatic cancer cells. *J Colloid Interface Sci.* 2010;351(1):19–29. doi:10.1016/j.jcis.2010.05.022
39. Acharya S, Sahoo SK. PLGA nanoparticles containing various anticancer agents and tumour delivery by EPR effect. *Adv Drug Deliv Rev.* 2011;63(3):170–183. doi:10.1016/j.addr.2010.10.008
40. Khan S, Chauhan N, Yallapu MM, et al. Nanoparticle formulation of ormeloxifene for pancreatic cancer. *Biomaterials.* 2015;53:731–743. doi:10.1016/j.biomaterials.2015.02.082
41. Hu C-MJ, Zhang L, Aryal S, Cheung C, Fang RH, Zhang L. Erythrocyte membrane-camouflaged polymeric nanoparticles as a biomimetic delivery platform. *Proc National Acad Sci.* 2011;108(27):10980–10985. doi:10.1073/pnas.1106634108
42. Kumari A, Yadav SK, Yadav SC. Biodegradable polymeric nanoparticles based drug delivery systems. *Colloids Surf B.* 2010;75(1):1–18. doi:10.1016/j.colsurfb.2009.09.001
43. Fang RH, Aryal S, Hu C-MJ, Zhang L. Quick synthesis of lipid-polymer hybrid nanoparticles with low polydispersity using a single-step sonication method. *Langmuir.* 2010;26(22):16958–16962. doi:10.1021/la103576a
44. Chowdhury P, Nagesh PKB, Hatami E, et al. Tannic acid-inspired paclitaxel nanoparticles for enhanced anticancer effects in breast cancer cells. *J Colloid Interface Sci.* 2019;535:133–148. doi:10.1016/j.jcis.2018.09.072
45. Hatami E, Nagesh PKB, Chowdhury P, et al. Tannic acid-lung fluid assemblies promote interaction and delivery of drugs to lung cancer cells. *Pharmaceutics.* 2018;10:3. doi:10.3390/pharmaceutics10030111
46. Mayor S, Pagano RE. Pathways of clathrin-independent endocytosis. *Nature Rev Mol Cell Biol.* 2007;8(8):603–612. doi:10.1038/nrm2216
47. Saavedra KP, Brebi PM, Roa JCS. Epigenetic alterations in preneoplastic and neoplastic lesions of the cervix. *Clin Epigenetics.* 2012;4(1):13. doi:10.1186/1868-7083-4-13
48. Bosch FX, Manos MM, Muñoz N, et al. Prevalence of human papillomavirus in cervical cancer: a worldwide perspective. *J Natl Cancer Inst.* 1995;87(11):796–802. doi:10.1093/jnci/87.11.796
49. Chichareon S, Herrero R, Muñoz N, et al. Risk factors for cervical cancer in Thailand: a case-control study. *J Natl Cancer Inst.* 1998;90(1):50–57. doi:10.1093/jnci/90.1.50
50. Ronco G, Segnan N. HPV testing for primary cervical cancer screening. *Lancet.* 2007;370(9601):1740–1742. doi:10.1016/S0140-6736(07)61480-9
51. Gillison ML, Chaturvedi AK, Lowy DR. HPV prophylactic vaccines and the potential prevention of noncervical cancers in both men and women. *Cancer.* 2008;113(S10):3036–3046. doi:10.1002/cncr.23764
52. Maeda H, Wu J, Sawa T, Matsumura Y, Hori K. Tumor vascular permeability and the EPR effect in macromolecular therapeutics: a review. *J Controlled Release.* 2000;65(1):271–284.
53. Yhee JY, Son S, Son S, Joo MK, Kwon IC. The EPR effect in cancer therapy. *Cancer Targeted Drug Delivery.* 2013;Chapter 23:621–632. doi:10.1007/978-1-4614-7876-8_23
54. Davis ME, Shin DM. Nanoparticle therapeutics: an emerging treatment modality for cancer. *Nature Rev Drug Discovery.* 2008;7(9):771–782. doi:10.1038/nrd2614
55. Gupta RC, Paliwal JK, Nityanand S, Asthana OP, Lal J. Centchroman: a new non-steroidal oral contraceptive in human milk. *Contraception.* 1995;52(5):301–305.
56. Gao H, Yang Z, Zhang S, et al. Ligand modified nanoparticles increases cell uptake, alters endocytosis and elevates glioma distribution and internalization. *Sci Rep.* 2013;3:2534. doi:10.1038/srep02534

International Journal of Nanomedicine

Dovepress

Publish your work in this journal

The International Journal of Nanomedicine is an international, peer-reviewed journal focusing on the application of nanotechnology in diagnostics, therapeutics, and drug delivery systems throughout the biomedical field. This journal is indexed on PubMed Central, MedLine, CAS, SciSearch[®], Current Contents[®]/Clinical Medicine,

Journal Citation Reports/Science Edition, EMBase, Scopus and the Elsevier Bibliographic databases. The manuscript management system is completely online and includes a very quick and fair peer-review system, which is all easy to use. Visit <http://www.dovepress.com/testimonials.php> to read real quotes from published authors.

Submit your manuscript here: <https://www.dovepress.com/international-journal-of-nanomedicine-journal>